



Synthesis of soluble oligo- and polymeric pentacene-based materials

Dan Lehnherr, Robert McDonald[†], Michael J. Ferguson[†], Rik R. Tykwinski^{*}

Department of Chemistry, University of Alberta, Edmonton, AB T6G 2G2, Canada

ARTICLE INFO

Article history:

Received 3 September 2008

Accepted 12 September 2008

Available online 24 September 2008

Dedicated to Professor Reginald H. Mitchell on the occasion of his 65th birthday

Keywords:

Pentacene

Oligomer

Polymer

π -Stacking

Organic semiconductor

Optoelectronic

Polycyclic aromatic hydrocarbon (PAH)

ABSTRACT

Functionalization of pentacene at the 6- and 13-positions affords versatile building blocks for oligomer and polymer formation. Di- and trimeric materials are synthesized using unsymmetrical building block **18**, while symmetrical diol monomer **17** allows for the synthesis of polymers. The materials reported herein are soluble in common organic solvents and air-stable. UV-vis and fluorescence spectroscopic properties have been investigated. Solid-state X-ray crystallography of building blocks **17** and **19** shows that these derivatives can π -stack with significant acene face-to-face interactions with spacing of less than 3.5 Å.

© 2008 Elsevier Ltd. All rights reserved.

1. Introduction

The last decade has seen an intensifying effort in the search for organic materials for optoelectronic applications. Today, the field of organic semiconducting materials is beginning to have a practical impact and offers the potential to revolutionize applications in photovoltaic cells, chemical sensors, thin film transistors (TFTs), as well as nanowire-based transistors.^{1–3} Organic materials can provide numerous advantages over their inorganic counterparts, including ease of tunability of the HOMO and LUMO levels through chemical functionalization, compatibility with flexible substrates, as well as lower manufacturing costs. The use of polycyclic aromatic hydrocarbons (PAHs), such as pentacene, has dominated most studies, but despite the substantial research on pentacene devices, relatively few derivatives of pentacene are known.^{1,4} Historically, efforts to enhance the performance of pentacene-based materials have been through device fabrication techniques rather than synthetic modifications of the pentacene skeleton. More recently, however, synthetic derivatization of the pentacene core has been

used to enhance the semiconductive properties (i.e., charge-carrier mobilities) and processability of pentacene-based materials.⁴ A natural progression in the development of organic advanced materials is the incorporation of functional chromophores into an oligo- and/or polymeric framework with the goal of increasing the solubility, as well as facilitating the formation of films and overall processability. In spite of their potential, however, pentacene-based oligomers and polymers remain rare.⁵

Unlike pentacene oligomers, anthracene oligomers are well known,^{6–11} and they often show improved electronic properties as a result of oligomerization.^{6–8,11} While the number of reports on anthracene oligomers is too large to summarize herein, Figure 1 highlights several examples. Suzuki and co-workers reported anthracene-based dimers **1–2** and trimers **3–4** in 2003, which were synthesized by Suzuki cross-coupling.⁶ Functionalization with solubilizing groups in dimer **2** and trimer **4** gave improved device performance in field effect transistors (FETs) in comparison to unfunctionalized oligomers **1** and **3**. In fact, oligomers **2** and **4** had FET mobilities of 0.13 and 0.18 cm² V⁻¹ s⁻¹, respectively. Conjugated anthracene trimer **5** was reported in 2008 by Suranna and co-workers and was synthesized by a Sonogashira cross-coupling to afford materials suitable for FETs with a mobility as high as 0.055 cm² V⁻¹ s⁻¹.⁷ Hybrid anthracene-thiophene oligomer **6** and tetracene-thiophene oligomer **7** were reported by Frisbie and co-workers and synthesized via Stille cross-coupling.⁸ Oligomers **6** and

^{*} Corresponding author. Tel.: +1 780 492 5307; fax: +1 780 492 8231.

E-mail address: rik.tykwinski@ualberta.ca (R.R. Tykwinski).

[†] X-ray Crystallography Laboratory, Department of Chemistry, University of Alberta.

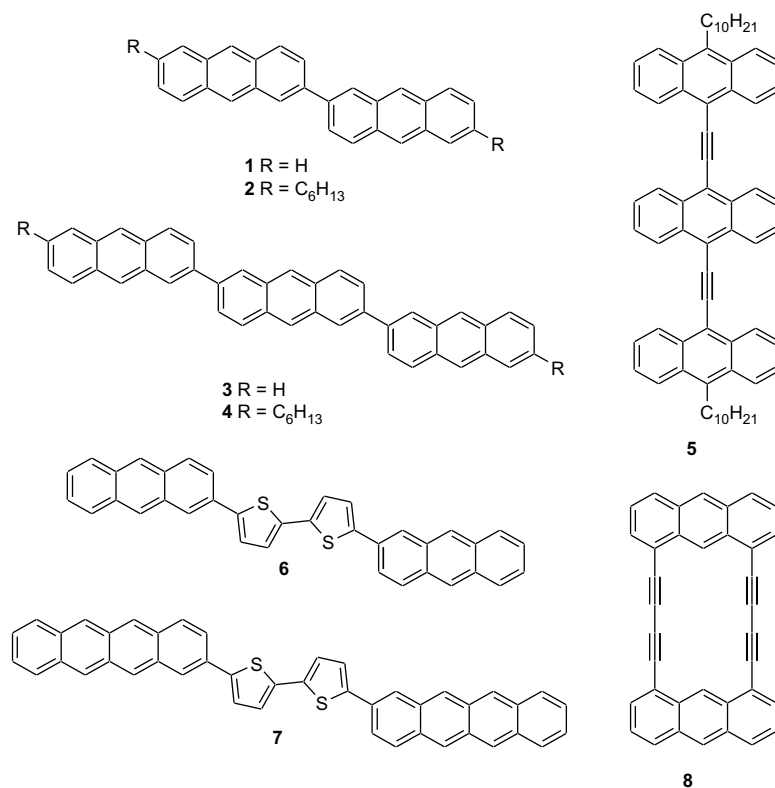


Figure 1. Selected examples of anthracene oligomers.

7 showed impressive performance in TFTs with hole mobilities as high as 0.1 and 0.5 cm² V⁻¹ s⁻¹, respectively. Various conjugated macrocyclic anthracenes have been studied by Toyota and co-workers, including di-, tri-, and tetramers, as well as the corresponding linear oligomers.⁹ And finally, even though cyclic anthracene dimer **8** has been known for half a century,¹⁰ it was only recently that Miao and co-workers studied its potential for applications in FETs.¹¹ FETs were fabricated via thermal deposition of **8** (due to its insoluble nature) and hole mobilities of 0.05 cm² V⁻¹ s⁻¹ were measured.

Tokito and co-workers first reported pentacene polymers in 2001.¹² The molecular structure of the random copolymers **9** was a composition of functionalized fluorene with pentacene present as either 1 or 10 mol % of the acene content (Fig. 2). The mixed acene polymers were synthesized using Ni(0)-mediated Yamamoto-coupling, and the materials were evaluated for their emissive properties. Conjugated pentacene polymers **10** and **11** were reported by Bao and Okamoto in 2007.¹³ In this case, the polymerization process was conducted at the pro-cata positions¹⁴ of the pentacene moiety, providing a mixture of the 2,9- and 2,10-isomeric linkages along the polymer backbone. Recently, the synthesis of conjugated pentacene dimers **12–14** has been reported by Tykewinski and Lehnher, in which dimer **14** exhibited photoconductive gain.¹⁵ There has been one report of non-conjugated pentacene-based oligo- and polymeric materials connected at the 6,13-positions (e.g., **15** and **16**) communicated in 2007.⁵ A full account of this work is presented herein.

2. Synthesis of pentacene-based materials

2.1. Synthesis of pentacene building blocks

Anthony and co-workers^{4a–e} have demonstrated that substitution of pentacene at the 6,13-positions with ethynylsilane groups improves stability versus pristine pentacene. It would

appear to be a combination of electronic and steric interactions that contribute to provide bench-top stable materials, although the exact nature of the electronic interaction has yet to be fully understood. Of the known pentacenes with 6,13-ethynylsilane substituents, triisopropylsilylethynyl is by far the most popular group for substitution of the pentacene chromophore due to its ability to afford stable, soluble pentacenes, which crystallize with significant face-to-face interaction.^{4a–e} These observations have been implemented in the design of a pentacene monomer for assembly into oligo- and polymers. Thus, building blocks **17** and **18** (Fig. 3) feature pendent Si-groups that serve as an attachment point for two isopropyl groups to enhance solubility and stability, as well as a 'functional arm' for polymerization. For the 'functional arm', a primary alcohol was chosen to allow for the formation of oligo- and polyesters via condensation reactions with either dicarboxylic acids or bis-acid chlorides.

The synthesis of **17** and **18** was envisioned from **19** (Fig. 3), which began by constructing the side groups in the form of a functionalized silylacetylene that derived from 4-bromobenzyl alcohol, **20**. Although **20** is commercially available, in this case it was made from 1,4-dibromobenzene (Scheme 1). Initial attempts to form the mono-Grignard of **21** in either THF or ether and quenching with paraformaldehyde gave unsatisfactory results (ca. 15% yield). As a result, the formation of a suitable aryl nucleophile via lithium/halogen exchange was attempted. Lithiation of **21** at –78 °C or even –40 °C was problematic due to the low solubility of the starting material. Success came by carrying out a mono-lithiation of **21** at –15 °C, even though not all of **21** was dissolved. Subsequent addition of paraformaldehyde to this solution gave **20** in a modest yield of 65% after recrystallization from CH₂Cl₂/hexanes. Alcohol **20** was then protected as the *tert*-butyldimethylsilyl (TBS) ether to give **22** in 90% yield using an adaptation of the procedure reported by Sessler and co-workers (CH₂Cl₂ or MeCN was used instead of DMF).¹⁶ Purification of **22** could conveniently be obtained via

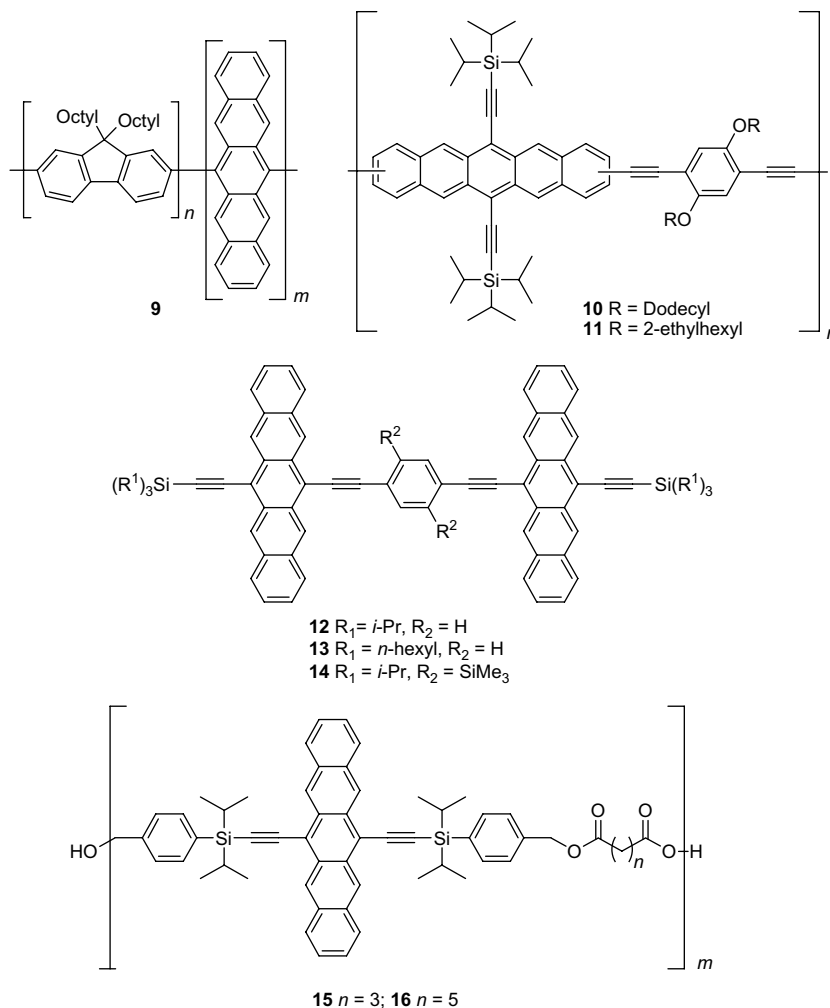


Figure 2. Pentacene oligo- and polymers.

reduced pressure distillation, thus avoiding the use of column chromatography.

Two routes were then explored toward the formation of **23**. Initially, a one-pot sequence was developed, in which **22** was subjected to lithium–halogen exchange with BuLi, and the product was then added to a solution of *i*-Pr₂SiCl₂ in THF at –78 °C. To this solution was added TMS–C≡C–Li, which afforded a ~2:1 mixture of **24** and **23** (as determined by ¹H NMR spectroscopy) in 62% overall yield after purification by reduced pressure distillation. Since the desired product in this case was **23**, the resulting mixture was subjected to mild desilylation conditions to provide the

terminal alkyne product in 58% (based on **22**) with no purification necessary other than aqueous work up.

A significant improvement in the synthesis of **23** was subsequently achieved using H–C≡C–MgBr instead of TMS–C≡C–Li

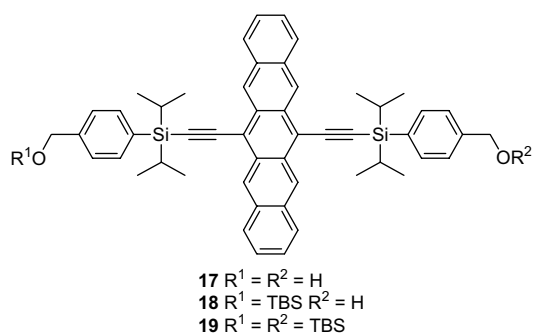
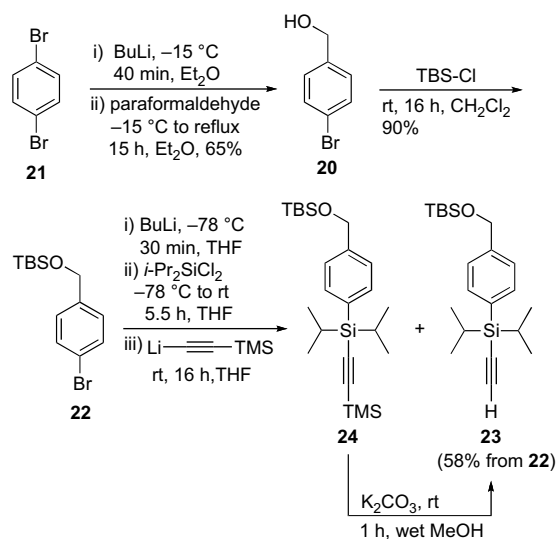
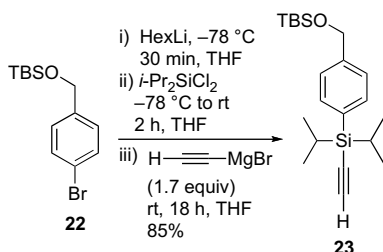


Figure 3. Pentacene building blocks 17–19.

Scheme 1. Synthesis of functionalized silylacteylene **23**.

(Scheme 2). Thus, lithiated **22** was added to a solution of *i*-Pr₂SiCl₂ in THF at $-78\text{ }^{\circ}\text{C}$. The resulting solution was then allowed to warm to room temperature and stir for 2 h. After again cooling the reaction mixture to $-78\text{ }^{\circ}\text{C}$, H-C≡C-MgBr was added and the resulting solution stirred at ambient temperature overnight. This



Scheme 2. Optimized synthesis of **23**.

sequence afforded directly **23** in 85% yield, circumventing the need for a desilylation step. It is worth noting that this route also makes use of less expensive reagents.

Both synthetic routes to **23** described above are scalable to tens-of-grams, and neither require column chromatography for any step starting from 1,4-dibromobenzene. This is obviously quite desirable when working on large-scale synthesis. In both synthetic routes, however, the quality of the *i*-Pr₂SiCl₂ plays a crucial role in the yield of this reaction. It is vital to use pure *i*-Pr₂SiCl₂ that has been stored under a rigorously inert atmosphere to prevent its degradation.

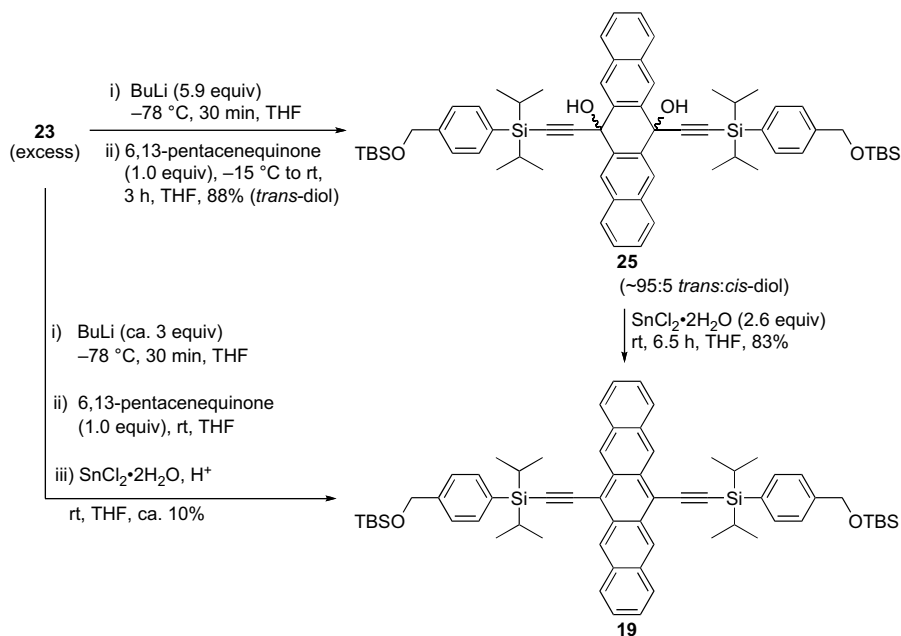
Initial attempts toward the synthesis of **19** employed a two-step, one-pot method analogous to that reported by Anthony and co-workers (Scheme 3).^{4a} Thus, **23** was lithiated and added to 6,13-pentacenequinone, followed by Sn(II)-mediated reduction. This gave **19** in very low yields (ca. 5–10%), and the isolated product consistently contained impurities. For example, **23** (3.7 equiv) was reacted with BuLi (3.0 equiv) in THF at $-78\text{ }^{\circ}\text{C}$, added to 6,13-pentacenequinone (1 equiv) at $0\text{ }^{\circ}\text{C}$, warmed to rt, and stirred for 2 h. The reaction was quenched with water followed by the addition of 10% HCl saturated with SnCl₂·2H₂O to give **19** as an impure blue-green solid after column chromatography. Attempts to improve the

process by either partial purification of the crude diol or by performing an aqueous work up prior to the Sn(II)-mediated reduction were ineffective. Lengthening the reaction time of the initial alkylation to 24 h did not improve the outcome. Likewise, increasing the temperature from ambient to refluxing temperatures did not yield better results either.

Given the challenges encountered during the attempted optimization of this two-step, one-pot procedure, this approach was ultimately abandoned in favor of a stepwise sequence in which the intermediate diol **25** was isolated and purified (Scheme 3). Using this approach, it was quickly realized that the main problem was that 3 to 3.5 equiv of the lithium acetylide derived from **23** was not sufficient to form **25** in good yield; a significant amount of monoaddition product **26** was observed (Fig. 4). This issue was resolved by using 5.9 equiv (2.9 equiv per ketone moiety) of the lithium acetylide. Further optimization in terms of reaction times and temperatures resulted in the conditions shown in Scheme 3.

Thus, under these optimized conditions a mixture of *cis*- and *trans*-diol **25** (~5:95 ratio) was formed, from which the *trans*-diol could be isolated in 88% yield by column chromatography. The *cis*-diol **25** could also be isolated (which was indeed done for characterization purposes), albeit the isolation process was tedious and time consuming because it has an *R_f* very similar to that of the major impurities/side products of the reaction. It is worth noting that the excess **23** could be recovered almost quantitatively (>90%) from this reaction during purification.

For the Sn(II)-mediated reduction of purified *trans*-diol **25**, the use of typical conditions^{4a} in THF or in a mixture of THF/CH₃CN under reflux failed to provide satisfactory results both in terms of yield and purity. Thus, milder conditions were sought, which included reducing the temperature (room temperature). The success of this step was solvent dependent, in terms of reaction rate, yield, and purity. For example, reactions at room temperature in CH₃CN or acetone were complete in less than 30 min, but numerous byproducts and low yields were encountered. Specifically, reactions in acetone gave up to 68% yield, while those in CH₃CN provided up to 64% yield. The presence of byproducts, however, made purification difficult and unsuitable for large-scale reactions. The reaction was also attempted in MeOH at room temperature, as well as



Scheme 3. Functionalization of pentacene to give **19**.

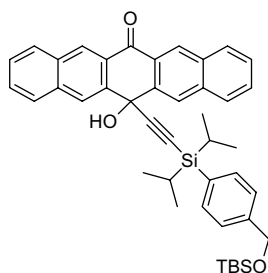


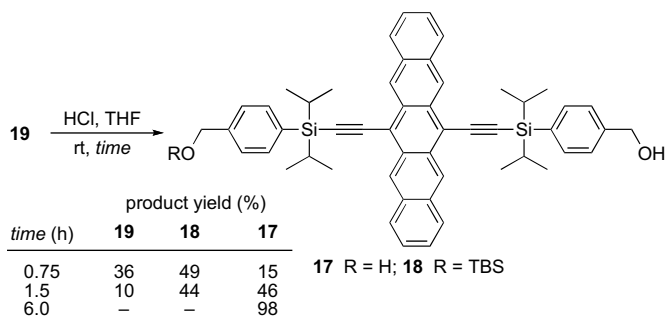
Figure 4. Structure of monoaddition product **26** isolated during the formation of **25**.

in 1:1 THF/CH₃CN (both at room temperature and accompanied by heating), but these also gave unsatisfactory results despite accelerating the rate of reaction.

Thus, best results were ultimately achieved by conducting the Sn(II)-mediated reduction of *trans*-diol **25** in THF at room temperature without HCl. The method gave protected monomer **19** in 83% yield as a blue solid. Over the course of attempts to optimize this process, it became clear that when diol **25** was exposed to SnCl₂·2H₂O in the presence of 10% HCl, loss of one or both of the TBS group(s) occurred and more complex product mixtures were produced. Thus, conditions that avoided the use of aq HCl for the Sn(II)-mediated reduction of diol **25** were employed and successfully prevented loss of the TBS protecting group.

2.2. Desymmetrization via kinetic desilylation

Removal of the two TBS groups to unveil the diol functionality of monomer **17** was accomplished in nearly quantitative yield using dilute HCl in THF (Scheme 4). If the reaction time was limited to 45 min, monodeprotected **18** was isolated in 49% yield, along with the recovery of 36% of unreacted **19** and 15% of diol **17**. All three compounds could be easily separated by column chromatography. Alternatively, extending the reaction time to 1.5 h gave nearly equal amounts of **17** (46%) and **18** (44%), along with 10% of unreacted **19**.



Scheme 4. Desilylation to obtain building blocks **17** and **18**.

2.3. Oligomerization process

Pentacene dimers **27–34** (Scheme 5) and trimers **35–36** (Scheme 6) were synthesized as model compounds to bridge the gap between monomer **17** and polymers **15** and **16**. The synthesis of pentacene-based oligomers made use of unsymmetrical pentacene building block **18**. Initially, solubility was a concern and, as a result, a pentacene dimer with a long alkyl tether linking the two ester groups was targeted. The dimerization process was first attempted in THF, with 1 equiv of 1,10-decanedioic acid chloride and 2 equiv of **18** in the presence of DMAP and Et₃N. This gave an unsatisfactory

yield of dimer **34** (ca. 15%); the major product isolated was the mono condensation product **37** (Fig. 5). Optimization was achieved by (a) switching to a more hydrophobic solvent (CH₂Cl₂), (b) using an excess of bis-acid chloride, (c) performing the reaction in a minimal amount of solvent (to provide higher concentrations of **18**), and (d) using only DMAP, rather than a mixture of Et₃N and DMAP. Ultimately, this led to an excellent yield for the dimerization process (79%).

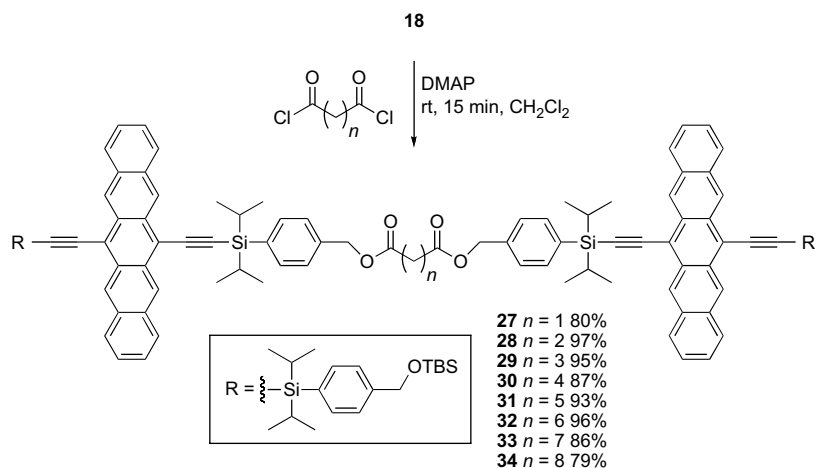
Dimer **34** was indeed readily soluble in a number of common organic solvents. Thus, synthesis of dimers with gradually shorter linkers was conducted, and dimers **27–34** with 1–8 methylene groups were synthesized in excellent yield (79–97%, Scheme 7). This allowed for a systematic study of the effects of tether length on solubility, aggregation, and thin film formation. All of the dimers were highly soluble in CH₂Cl₂, CHCl₃, and THF, although those with shorter linkers (*n*=1 and 2) had slightly reduced solubility in comparison to other dimers.

Pentacene trimers were then synthesized using desymmetrized pentacene **18** to react with succinic or glutaric anhydride affording **38** and **39** with a pendent carboxylic acid group (Scheme 6). Initially, work up to remove the excess anhydride (along with DMAP) included washing with satd aq NaHCO₃, followed by 5% aq NaHCO₃, and then satd aq NaCl. It was determined, however, that basic conditions should be avoided to circumvent the possible formation of the sodium carboxylate salt during work up. The formation of **38** and **39** also typically gave a trace of the corresponding dimer (ca. <5%) via an additional coupling of the product under the reaction conditions. This byproduct could be easily removed by size exclusion chromatography to afford the pure carboxylic acids **38** and **39**. Alternatively, the byproduct could be separated after formation of trimer **35** or **36**, at which point the difference in *R_f* values allowed separation using column chromatography on silica gel.

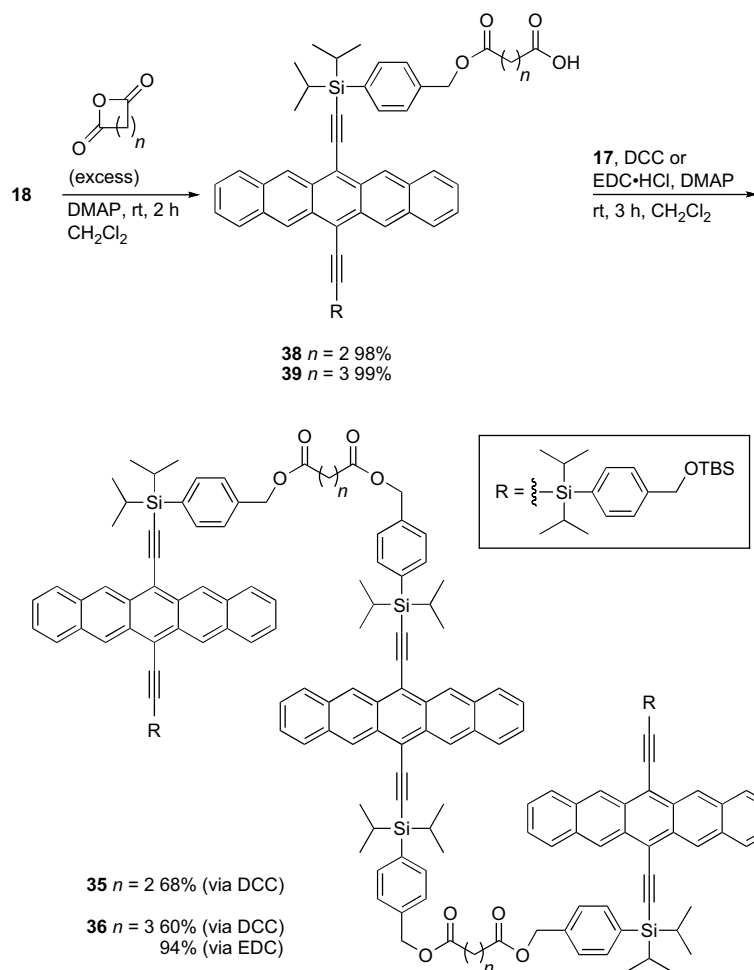
A subsequent DCC mediated coupling of acid **38** or **39** with monomer **17** afforded trimers **35** and **36**. It was subsequently determined that the synthesis of trimers could be simplified by substituting EDC·HCl for DCC. This change in reagent greatly facilitated purification by virtue of forming water-soluble byproducts, and it also eliminated the need for product purification by size exclusion chromatography. For example, EDC mediated coupling gave trimer **36** in 94% yield. The EDC method was also explored for the synthesis of one dimer (*n*=2), and gave **28** in similar yield (90%) as the bis-acid chloride method.

With a series of dimers and trimers in hand, polymers **15** and **16** were targeted, and a number of polymerization conditions were explored during optimization of their synthesis (Scheme 7). Initially, slow addition of a solution of the requisite bis-acid chloride **40** or **41** to a solution of **17** (~5×10⁻³ M) in the presence of DMAP was tried, but this resulted in formation of a significant quantity of cyclic oligomers, as determined by mass spectrometry analysis. Reversing the order of addition (i.e., adding monomer **17** to a solution of **40** or **41** in the presence of DMAP) led to the isolation of primarily unreacted **17**, seemingly due to quenching of the acid chloride by adventitious water. Polymerization of **17** using the corresponding bis-carboxylic acids and coupling agents such as EDC·HCl in the presence of DMAP also gave significant amounts of cyclic oligomers.

Ultimately, polymerization was best accomplished by preparing a suspension of monomer **17** with DMAP in CH₂Cl₂ (~5×10⁻² M) and quickly adding a solution of **40** or **41**. Following aqueous work up, purification of **15** and **16** could be effected simply by recrystallization. MALDI mass spectrometry (MS) analysis showed macromolecules of over *m/z* 17,000 were achieved (e.g., *m*=20) for **15** and over *m/z* 15,000 (*m*=17) for **16**. More specifically, this analysis showed a distribution of oligomers from *m*=2 to 20 and beyond for polymer **15**, while the spectrum



Scheme 5. Synthesis of a homologous series of pentacene dimers.

Scheme 6. Synthesis of trimers **35** and **36**.

for polymer **16** showed signals for $m=2$ to 17 and beyond. In addition to the generalized polymer structure shown in Scheme 7 for **15** and **16** (terminated with an acid and an alcohol), the product mixtures also consisted of structures terminated with two acids, two alcohols, and macrocyclic structures resulting from intramolecular ester formation.¹⁷

3. UV-vis and fluorescence spectroscopy

UV-vis spectra of the new pentacene materials have been measured in CH_2Cl_2 . Figure 6 shows the absorption spectrum of protected monomer **19**, which is representative of all the derivatives studied. A strong absorption is observed at $\lambda_{\text{max}}=309$ nm

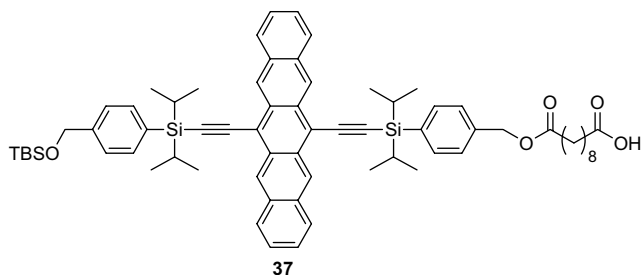


Figure 5. Moncondensation side-product **37**.

along with a series of low-energy absorptions, with the lowest energy having a λ_{\max} at 645 nm. Compared to pristine pentacene, which has λ_{\max} =584 nm in ethanol¹⁸ and λ_{\max} =576 nm in benzene,¹⁹ this represents a red-shift of \sim 65 nm.

Solvatochromism studies have been carried out for the more diversely soluble pentacene **19** (Table 1) and small changes in the position of λ_{\max} for the absorption bands are observed. Focusing on the lowest energy λ_{\max} , one observes that the transition is most red-shifted in CH_2Cl_2 , CHCl_3 , and toluene, whereas the band is most blue-shifted in hexanes, cyclohexane, and ethanol. In terms of ϵ for the various bands as a function of solvent, minor changes are observed. Molar absorptivity coefficients (ϵ) in non-polar solvents such as hexanes and cyclohexane were higher for both the high-energy band as well as the low-energy transitions. On the other hand, compared to the remaining solvents in the table, toluene produces lower ϵ values for the high-energy absorption at 310 nm, without yielding lower ϵ values for the low-energy absorptions. No correlation was observed for either λ_{\max} or ϵ as a function of the hydrogen-bonding capacity or the polarity of the solvent.

The electronic structure of this basic pentacene unit found in, for example **19**, is essentially unaffected by oligomer or polymer formation. Comparing the UV-vis spectra of the homologous series made up of monomer **19**, dimer **29**, trimer **36**, and polymer **15** reveal that all molecules share nearly identical absorption maxima (± 1 nm) (Table 2 and Fig. 7). Molar absorptivity coefficients (ϵ) change monotonically as a function of oligomer length (Table 2). In fact, a plot of ϵ as a function of the number of pentacene chromophores present in the molecule is essentially linear. For example, this analysis has been made for monomers **17**–**19** in comparison to dimers **27**–**34** and trimers **35**–**36** at 309 nm and 645 nm, and both result in linear fits with $R^2=0.991$ and $R^2=0.992$, respectively.²⁰ Thus, there appears to be no intramolecular self-association of the pentacene moieties of these oligomers in solution.

The absorption spectra of polymers **15** and **16** have been examined as thin films cast onto fused silica from CH_2Cl_2 . In each case, the low-energy absorptions between 475 and 675 nm are slightly

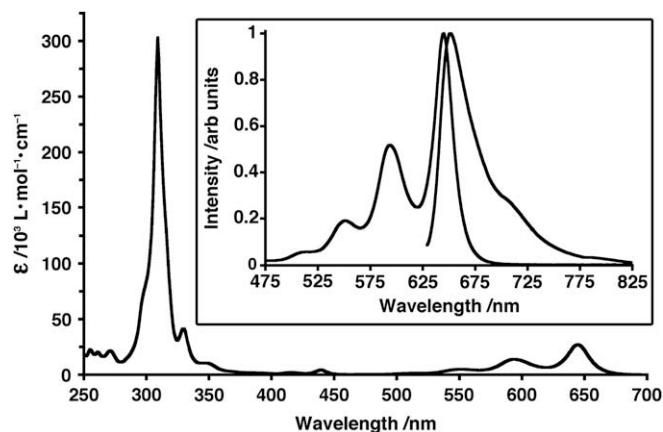


Figure 6. UV-vis of **19** in CH_2Cl_2 representative of pentacene materials presented herein. Inset: low-energy absorption region (right hand side trace), and fluorescence using $\lambda_{\text{exc}}=309$ nm (left hand side trace) normalized to unity.

red-shifted (<10 nm) in comparison with those measured in solution.²¹

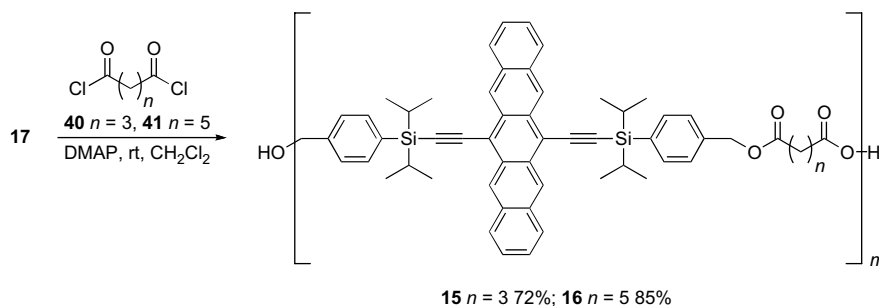
The emission of the pentacene materials has been investigated in CH_2Cl_2 (Table 3). The fluorescence spectrum of **19** is representative, and shows a broad and relatively featureless emission with $\lambda_{\max,\text{em}}=652$ nm ($\lambda_{\text{exc}}=309$ nm, Fig. 6). This represents a small Stokes shift of only 7 nm and suggests minimal molecular rearrangement occurs upon photoexcitation of the molecule. A plot of normalized fluorescence traces ($\lambda_{\text{exc}}=551$ nm) for all these materials (Fig. 8) demonstrates that the overall emission profiles are essentially identical.

Fluorescence quantum yields, Φ_F , for all derivatives were measured using cresyl violet perchlorate as a standard,²² and the results are summarized in Table 3. While Φ_F seems to vary somewhat for the three monomeric pentacenes **19**, **17**, and **18** ($\Phi_F=0.08$ – 0.17), all dimers, and both trimers show very similar Φ_F values. Specifically the dimers all tend to be around $\Phi_F=0.08$ – 0.11 , whereas the values for the trimers, $\Phi_F=0.06$, are about half that of the dimers.

Further analysis of Φ_F data for dimers **27**–**34** suggests that the length of the methylene tether between the two pentacene chromophores might exert a small effect on fluorescence efficiency: the longer the tether, the larger the Φ_F (excluding **27**). Ultimately, however, this effect is on the same order of magnitude as the expected error in the measurements (ca. 10%), so this correlation is somewhat tenuous.

4. Aggregation

In dilute solutions, as used for UV-vis spectroscopy ($\sim 10^{-5}$ to 10^{-6} M), Beer's Law is maintained for dimers **27**–**34**. For example, a plot of absorption at $\lambda_{\max}=645$ nm as a function of concentration



Scheme 7. Synthesis of polymers **15** and **16**.

Table 1
Solvatochromism study of pentacene **19**

Solvent	λ/nm ($\epsilon/\text{L mol}^{-1} \text{cm}^{-1}$)						
Hexanes	269 (27,700)	306 (322,000)	327 (48,300)	438 (4840)	543 (6060)	585 (17,600)	637 (40,000)
1-Butanol ^a	270	307	328	439	546	588	639
Cyclohexane	270 (27,300)	307 (304,000)	328 (47,000)	439 (4500)	545 (5740)	586 (17,300)	639 (39,600)
Ethyl acetate	269 (26,100)	306 (324,000)	328 (42,300)	439 (4570)	548 (5320)	589 (14,700)	640 (29,500)
Acetone	— ^b	— ^b	327 (42,000)	439 (4430)	548 (5150)	590 (13,900)	640 (26,800)
Acetonitrile ^a	269	306	328	439	549	592	641
Tetrahydrofuran	270 (28,600)	308 (305,000)	329 (43,500)	439 (5120)	549 (5730)	592 (15,500)	643 (31,000)
Toluene	— ^b	310 (214,000)	330 (43,700)	441 (4460)	550 (4990)	594 (14,300)	645 (28,800)
Chloroform	271 (23,900)	310 (266,000)	330 (41,300)	440 (4340)	551 (5120)	593 (14,300)	645 (28,400)
Dichloromethane	271 (21,500)	309 (303,000)	330 (41,300)	440 (4430)	551 (5000)	594 (13,900)	645 (27,100)
Largest change in $\lambda_{\text{max}}/\text{nm}$	2	4	3	2	8	9	8
Largest change in $\epsilon/\text{L mol}^{-1} \text{cm}^{-1}$	7200	110,000	7000	780	1070	3700	13,200
Largest percent change in $\epsilon/\%$	25	34	14	15	18	21	33

^a Denotes solution of unknown concentration due to low solubility, solution was filtered to remove undissolved solids prior to measurement.

^b Peak could not be measured accurately due to UV-vis cut-off for the solvent.

Table 2
UV-vis data for pentacene materials in CH_2Cl_2

Compound	Number of pentacene units	$\lambda_{\text{max}}/\text{nm}$ ($\epsilon/\text{L mol}^{-1} \text{cm}^{-1}$)						
17 , Monomer	1	271 (22,600)	309 (285,000)	330 (40,200)	440 (4330)	551 (4940)	594 (13,400)	645 (25,900)
18 , Pseudo monomer	1	271 (24,400)	309 (279,000)	329 (40,200)	440 (4240)	551 (4860)	593 (13,400)	644 (25,800)
19 , Protected monomer	1	271 (21,500)	309 (303,000)	330 (41,300)	440 (4430)	551 (5000)	594 (13,900)	645 (27,100)
27 , Dimer $n=1$	2	271 (45,600)	309 (536,000)	330 (78,500)	440 (8310)	552 (9600)	594 (26,200)	645 (50,400)
28 , Dimer $n=2$	2	271 (45,800)	309 (508,000)	330 (73,400)	440 (7500)	551 (8660)	593 (24,400)	645 (47,100)
29 , Dimer $n=3$	2	271 (46,500)	309 (547,000)	330 (79,800)	440 (8410)	551 (9690)	594 (26,600)	645 (51,100)
30 , Dimer $n=4$	2	271 (46,700)	309 (523,000)	329 (75,800)	440 (8090)	550 (9190)	593 (25,200)	644 (48,500)
31 , Dimer $n=5$	2	271 (46,400)	309 (540,000)	330 (78,800)	440 (8340)	552 (9620)	594 (26,300)	645 (50,600)
32 , Dimer $n=6$	2	271 (44,800)	309 (514,000)	330 (73,000)	440 (7360)	552 (8570)	594 (24,300)	645 (47,100)
33 , Dimer $n=7$	2	271 (41,800)	309 (531,000)	330 (74,900)	440 (6940)	552 (8550)	594 (24,900)	645 (48,800)
34 , Dimer $n=8$	2	271 (40,200)	309 (512,000)	330 (72,100)	440 (6690)	552 (8240)	594 (24,000)	645 (47,000)
35 , Trimer $n=2$	3	271 (66,900)	309 (802,000)	330 (113,000)	440 (12,200)	551 (13,700)	594 (37,700)	645 (72,400)
36 , Trimer $n=3$	3	271 (62,400)	309 (803,000)	330 (111,000)	440 (11,700)	551 (13,400)	594 (37,000)	645 (71,400)
15 , Polymer $n=3$	—	271	309	330	440	552	594	645
16 , Polymer $n=5$	—	271	309	330	440	552	594	645

for **28** (6.6×10^{-7} to 1.7×10^{-5} M) affords a linear best-fit line with R -value of 0.9998. Dimers with shorter linker chains (**27**, **31**, and especially **28**), however, aggregate in more concentrated solutions (ca. >0.05 M) as determined by ^1H NMR spectroscopy. In these

cases, multiple signals are observed where a single resonance is expected (Fig. 9). For example, the singlet observed for the *t*-Bu group of the TBS ether group is split into multiple signals. Upon dilution of the NMR sample, these resonances coalesce into a single

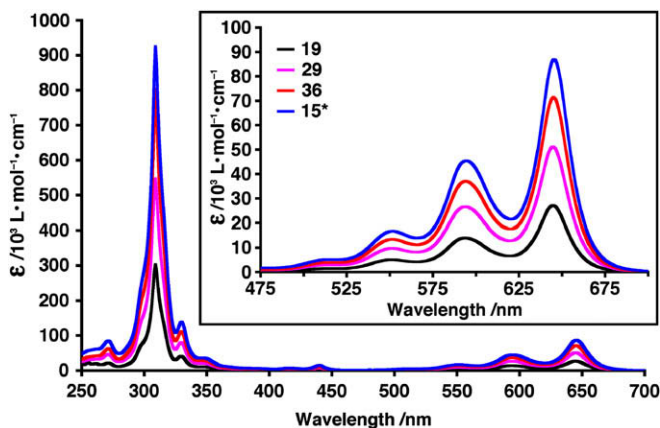


Figure 7. Effect of the oligomerization process on the UV-vis spectra of pentacene materials **19**, **29**, **36**, and **15** (in CH_2Cl_2). The intensity of the absorption trace for polymer **15** is plotted in arbitrary units.

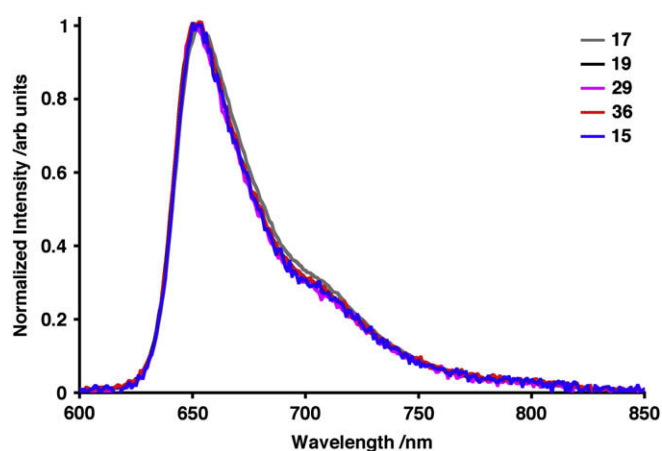


Figure 8. Fluorescence spectra of selected pentacenes in CH_2Cl_2 measured with $\lambda_{\text{exc}}=551$ nm (intensity normalized to unity).

Table 3
Summary of ϕ_F of pentacene materials in CH_2Cl_2 measured using $\lambda_{\text{exc}}=551\text{ nm}$

Compound	ϕ_F	$\lambda_{\text{max,em}}/\text{nm}$	Stokes shift/nm
17, Monomer	0.14	653	6
18, Pseudo monomer	0.17	652	8
19, Protected monomer	0.08	652	7
27, Dimer $n=1$	0.09	652	7
28, Dimer $n=2$	0.08	652	7
29, Dimer $n=3$	0.08	652	7
30, Dimer $n=4$	0.09	652	8
31, Dimer $n=5$	0.09	652	7
32, Dimer $n=6$	0.10	652	7
33, Dimer $n=7$	0.11	652	7
34, Dimer $n=8$	0.11	652	7
35, Trimer $n=2$	0.06	652	7
36, Trimer $n=3$	0.06	652	7

signal. Interestingly, no such similar aggregation behavior is observed in either the trimers or the polymers.

5. Thermal analysis

Differential scanning calorimetry (DSC) and thermal gravimetric analysis (TGA) have been carried out on most of the pentacene materials presented herein to assess thermal stability (Table 4).²³ Thermal stability as assessed by TGA shows no significant weight loss (<5%) below 350 °C in all cases. The oligomerization process increases the thermal stability slightly: monomer **17** shows decomposition at 365 °C, while all oligomers decompose above this temperature. This is perhaps a result of reducing the ratio of primary alcohols (nucleophilic) to pentacene moieties. Further support for this premise is provided by the fact that both **18** and **19**, which have either one or both alcohol moieties protected as the TBS ether, show higher thermal stability in comparison to monomer **17**. DSC analysis shows no glass transition temperature for polymers **15** and **16**. Additionally, no thermal event is observed in the DSC analysis below 350 °C for these materials, which could be associated with decomposition. This contrasts the behavior of closely related monomeric pentacene materials that show decomposition well below this temperature.^{4m,24}

6. X-ray crystallography

Solid-state packing plays an important role for materials in molecular electronics because electronic performance is often enhanced by strong electronic coupling mediated by strong intermolecular interactions between adjacent molecules.^{1–3} The solid-state structure of the common building block, **17**, has been determined by X-ray analysis of crystals grown from THF/MeOH.²⁵

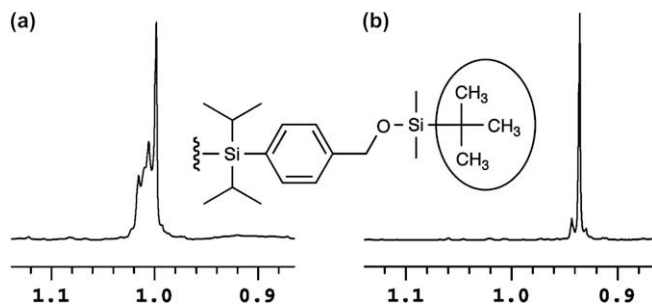


Figure 9. ^1H NMR signal corresponding to *t*-Bu of TBS group in **27** at a concentration of (a) $\sim 0.06\text{ M}$ (b) $\sim 0.002\text{ M}$ demonstrating the spectroscopic effects of aggregation in CDCl_3 .

Table 4
Thermal stability of pentacene materials determined by TGA and DSC

Compound	TGA $T_d/^\circ\text{C}$	DSC (decomposition)	
		Onset/ $^\circ\text{C}$	Maximum/ $^\circ\text{C}$
17, Monomer	365	325	375
18, Pseudo monomer	385	360	380
19, Protected monomer	385	380	395
27, Dimer $n=1$	370	370	390
28, Dimer $n=2$	390	380	395
29, Dimer $n=3$	385	360	390
30, Dimer $n=4$	400	370	405
31, Dimer $n=5$	385	375	395
32, Dimer $n=6$	400	370	390
33, Dimer $n=7$	385	380	395
34, Trimer $n=8$	385	375	395
35, Trimer $n=2$	380	370	390
36, Trimer $n=3$	380	365	390
15, Polymer $n=3$	385	370	405
16, Polymer $n=5$	380	370	385

Monomer **17** co-crystallizes with two molecules of MeOH (Fig. 10a). Analysis of the solid-state packing for **17** reveals molecules arranged in one-dimensional slipped-stacks (Fig. 12a),²⁶ with an interplanar distance between the acenes of 3.41 Å.²⁷ Thus, in terms of π -overlap and orientation in the solid-state, compound **17** is well suited for intermolecular communication.

Attempts have been made to obtain solvent free crystals of **17**, but these efforts have been unsuccessful to date. Nevertheless, an additional polymorph of **17** has been produced from a mixture of CH_2Cl_2 and acetone.²⁸ This results in a solid-state arrangement of two structurally independent molecules of **17**, namely molecules A (Fig. 10b) and molecule B (Fig. 10c). These two molecules are linked by hydrogen-bonding between their benzylic alcohol groups, additionally molecule A hydrogen bonds to an acetone solvent molecule (Fig. 11). The polymorph of **17** co-crystallized with acetone is also arranged in a one-dimensional slipped-stack configuration (Fig. 12b), with an interplanar distance between the acenes of 3.39 Å (molecule A to molecule A) and 3.45 Å (molecule B to molecule B). Since the individual one-dimensional stacks are formed exclusively from either molecules A or molecules B, no π -stacking interactions are found between molecules A and B in the solid-state.

Single crystals of **19** have been grown at 4 °C by allowing a CH_2Cl_2 solution of **19** layered by a small amount of acetone to evaporate slowly.²⁹ Although disorder is apparent in the *tert*-butyldimethylsilyloxybenzyl group of **19**, the remainder of the structure, including the bis-ethynylpentacene moiety, is uniformly arranged. Pentacene **19** reveals a two-dimensional slipped-stacks arrangement similar to that of pentacene derivatives exhibiting high hole mobility (Fig. 13).^{1–3,30} The interplanar distance between the acenes is 3.38 Å, which is slightly less than those in the polymorphs of **17**. These intermolecular distances in both polymorphs of **17** and **19** between the acenes are comparable to 6,13-bis(triisopropylsilylethynyl)pentacene, which has spacing of 3.47 Å.^{4a}

7. Conclusions

In conclusion, we provide a full account of the first reported synthesis of defined-length pentacene oligomers and representative polymeric derivatives, as well as a description of their physical properties. All molecules exhibit good solubility and stability. The synthetic strategy that has been developed is also amenable to inclusion of other terminal groups on the monomer unit that enables the synthesis of various other types of polymers and these results will be presented in due course.

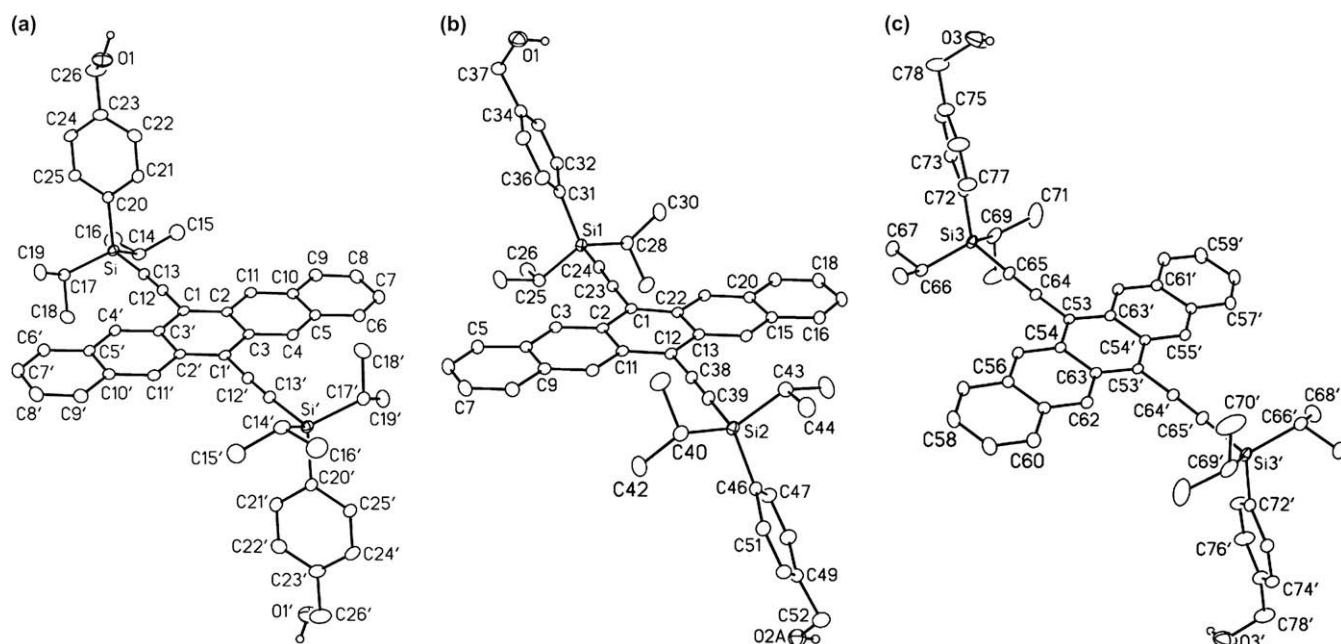


Figure 10. X-ray of **17** (a) polymorph grown from THF/MeOH. The polymorph of **17** grown from CH_2Cl_2 /acetone showing the two structurally independent geometries, (b) molecule A, and (c) molecule B.

8. Experimental section

8.1. General experimental

Reagents were purchased in reagent grade from commercial suppliers and used without further purification. Preliminary experimental procedures and spectroscopic data for compounds **15–20** and **22–39** have been previously reported.⁵ Detailed experimental procedures and spectroscopic data for compounds **15–20**, **22–25**, **27–36**, **38–39**, and spectroscopic data for **26** and **37** are provided as [Supplementary data](#). 6,13-Pentacenequinone³¹ was recrystallized from *N,N*-dimethylformamide, washed with dry THF, and dried under vacuum prior to use. THF and Et_2O were distilled from sodium/benzophenone ketyl; CH_3CN and CH_2Cl_2

were distilled from CaH_2 . Anhydrous MgSO_4 was used as the drying agent after aqueous work up. Evaporation and concentration in vacuo were done at water-aspirator pressure. All reactions were performed in standard, dry glassware under an inert atmosphere of nitrogen.

8.2. Synthesis of polymers **15** and **16**

8.2.1. Synthesis of polymer **15**

Compound **17** (0.105 g, 0.137 mmol), freshly recrystallized from CH_2Cl_2 /hexanes, was dissolved in dry CH_2Cl_2 (2.5 mL) and DMAP (0.080 g, 0.65 mmol) was added. To this mixture under stirring, a solution of **40** (0.27 M, 0.28 mL, 0.077 mmol), prepared from **40** (0.46 g, 0.35 mL, 2.7 mmol) dissolved in dry CH_2Cl_2 (10 mL), was quickly added. After ca. 30 s, a second portion of the solution of **40** (0.27 M, 0.25 mL, 0.069 mmol) was quickly added. The reaction mixture was then allowed to stir for 3 h before being diluted with CH_2Cl_2 (50 mL) and satd aq NaHCO_3 (100 mL). The mixture was separated and the organic phase was washed with 5% aq NaHCO_3 (1×100 mL), satd aq NH_4Cl (2×150 mL), satd aq NaCl (150 mL), and dried (MgSO_4). The solvent was removed in vacuo. The residue was dissolved in CH_2Cl_2 (2 mL) and precipitated by adding hexanes (40 mL) and cooling to -78°C . After filtering, the resulting solid was washed with hexanes (3×15 mL) and redissolved in CH_2Cl_2 . This solution was filtered through a fritted funnel to remove any undissolved solids, concentrated in vacuo, and the resulting solid dried under vacuum to afford polymer **15** (0.087 g, 72%) as a deep blue solid. UV-vis (CH_2Cl_2) λ_{max} : 271, 309, 330, 440, 552, 594, 645 nm. IR (CDCl_3 , cast) 3042 (w), 3020 (w), 2943 (s), 2864 (s), 2136 (m), 1738 (s) cm^{-1} . ^1H NMR (500 MHz, CDCl_3): δ 9.35 (br s, 4H), 7.99–7.94 (m, 4H), 7.88 (br d, $J=7.9$ Hz, 4H), 7.46–7.38 (m, 8H), 5.17 (br s, 4H), 2.47 (t, $J=7.4$ Hz, 4H), 2.04 (quintet, $J=7.3$ Hz, 2H), 1.61–1.48 (m, 4H), 1.38 (br d, $J=7.3$ Hz, 12H), 1.25 (d, $J=7.4$ Hz, 12H). ^{13}C NMR (125 MHz, CDCl_3): δ 172.7, 137.1, 135.6, 133.4, 132.4, 130.7, 128.6, 127.5, 126.2, 118.2, 105.9, 105.3, 66.2, 33.3, 20.1, 18.2, 18.1, 12.0. TGA: $T_d \approx 385^\circ\text{C}$. DSC: decomposition, 370°C (onset) and 405°C (peak).

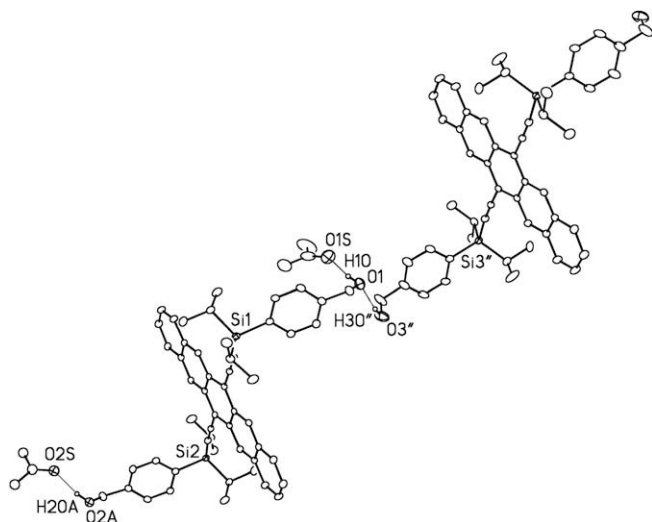


Figure 11. Hydrogen-bonding interactions between adjacent molecule A (left) and molecule B (right) of **17** and solvent acetone in crystals of **17** grown from CH_2Cl_2 /acetone.

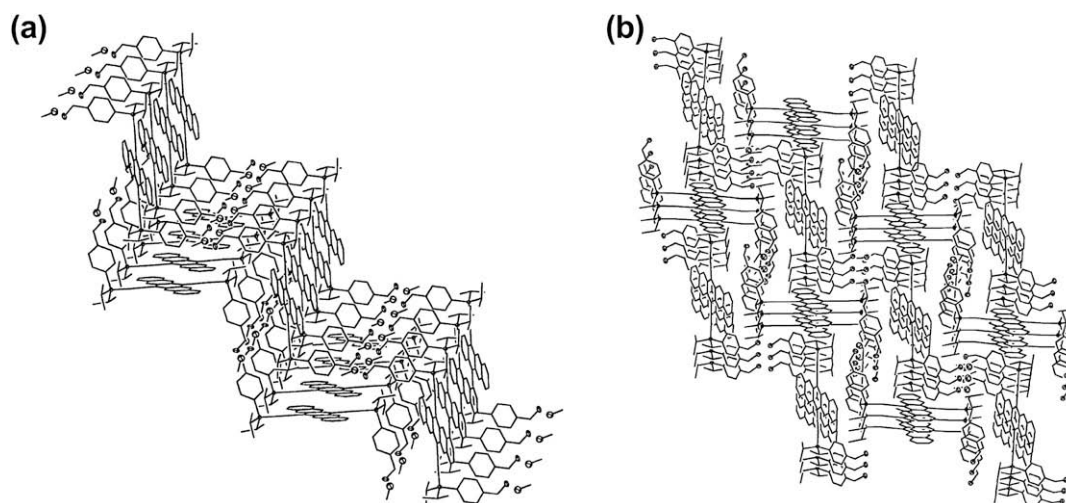


Figure 12. Solid-state packing of **17** from crystals grown from (a) THF/MeOH (b) CH_2Cl_2 /acetone (thermal ellipsoids for the carbon atoms have been omitted for clarity).

8.2.2. Synthesis of polymer **16**

Compound **17** (0.205 g, 0.261 mmol), freshly recrystallized from CH_2Cl_2 /hexanes, was dissolved in dry CH_2Cl_2 (5 mL) and DMAP (0.159 g, 0.130 mmol) was added. To this mixture under stirring, a solution of **41** (0.56 M, 0.50 mL, 0.28 mmol), prepared from **41** (0.55 g, 0.46 mL, 2.8 mmol) dissolved in dry CH_2Cl_2 (5 mL), was added dropwise over a period of 20 min. The reaction mixture was then allowed to stir for 2 days before being diluted into CH_2Cl_2 (50 mL) and satd aq NaHCO_3 (100 mL). The mixture was separated and the organic phase was washed with 5% aq NaHCO_3 (3×100 mL), satd aq NaCl (150 mL), and dried (MgSO_4). The solvent was removed in vacuo. The residue was dissolved in CH_2Cl_2 (2 mL) and precipitated by adding hexanes (40 mL) and cooling to -78 °C. After filtering, the resulting solid was washed with hexanes (3×10 mL) and redissolved in CH_2Cl_2 . This solution was filtered through a fritted funnel to remove any undissolved solids, concentrated in vacuo, and the resulting solid dried under vacuum to afford polymer **16** (0.202 g, 85%) as a deep blue solid. UV-vis (CH_2Cl_2) λ_{max} : 271, 309, 330, 440, 552, 594, 645 nm. IR (CDCl_3 , cast)

3045 (w), 2943 (s), 2890 (m), 2863 (m), 2136 (m), 1738 (s) cm^{-1} . ^1H NMR (500 MHz, CDCl_3): δ 9.32 (br s, 4H), 7.96–7.90 (m, 4H), 7.88 (br d, $J=7.9$ Hz, 4H), 7.42–7.35 (m, 8H), 5.12 (br s, 4H), 2.35 (t, $J=7.5$ Hz, 4H), 1.69–1.60 (m, 4H), 1.59–1.47 (m, 4H), 1.36 (br d, $J=7.4$ Hz, 12H), 1.39–1.31 (2H, this signal overlaps a broad doublet at 1.36), 1.22 (d, $J=7.4$ Hz, 12H). ^{13}C NMR (125 MHz, CDCl_3): δ 173.3, 137.3, 135.5, 133.2, 132.4, 130.7, 128.6, 127.4, 126.2, 118.2, 105.8, 105.3, 66.0, 34.0, 28.5, 24.5, 18.2, 18.1, 12.0. TGA: $T_d \approx 380$ °C. DSC: decomposition, 370 °C (onset) and 385 °C (peak).

8.3. Synthesis of dimers **27–34**

As a general procedure for the synthesis of pentacene-based dimers, procedures for **28** are presented as examples. The other syntheses are analogous and details are provided in Supplementary data.

8.3.1. Synthesis of **28** using succinyl chloride

Compound **18** (0.075 g, 0.085 mmol) was dissolved in dry CH_2Cl_2 (2 mL) and DMAP (0.0258 g, 0.211 mmol) was added. To this mixture under stirring, a solution of succinyl chloride (0.17 M, 0.25 mL, 0.042 mmol), prepared from succinyl chloride (0.13 g, 0.094 mL, 0.85 mmol) dissolved in dry CH_2Cl_2 (5 mL), was added dropwise over a period of 5 min. The reaction mixture was allowed to stir at rt for 3 min before adding additional solution of succinyl chloride (0.17 M, 0.25 mL, 0.042 mmol) dropwise followed by dry CH_2Cl_2 (5 mL). The reaction mixture was allowed to stir for 5 min before being diluted with dry CH_2Cl_2 (20 mL) and 5% aq NaHCO_3 (20 mL). The mixture was separated and the organic phase was washed with satd aq NaCl (25 mL), dried (MgSO_4), and the solvent removed in vacuo. Column chromatography (silica gel, CH_2Cl_2) afforded **28** (0.0757 g, 97%) as a deep blue solid.

8.3.2. Synthesis of dimer **28** using EDC·HCl

Compound **18** (0.156 g, 0.177 mmol), EDC·HCl (0.169 g, 0.855 mmol), and succinic acid (0.010 g, 0.085 mmol) were dissolved in dry CH_2Cl_2 (4 mL) and DMAP (0.108 g, 0.855 mmol) was added. The reaction mixture was allowed to stir at rt for 8 h before being poured into 5% aq NaHCO_3 (100 mL), which was then diluted with CH_2Cl_2 (50 mL). The mixture was separated and the organic phase was washed with 5% aq NaHCO_3 (100 mL), satd aq NaCl (150 mL), dried (MgSO_4), and the solvent removed in vacuo. Column chromatography (silica gel, CH_2Cl_2) afforded **28** (0.141 g, 90%) as a deep blue solid. $R_f=0.65$ (CH_2Cl_2). UV-vis (CH_2Cl_2) λ_{max} (ϵ): 271 (45,800), 309 (508,000), 330 (73,400), 440 (7500), 551 (8660), 593

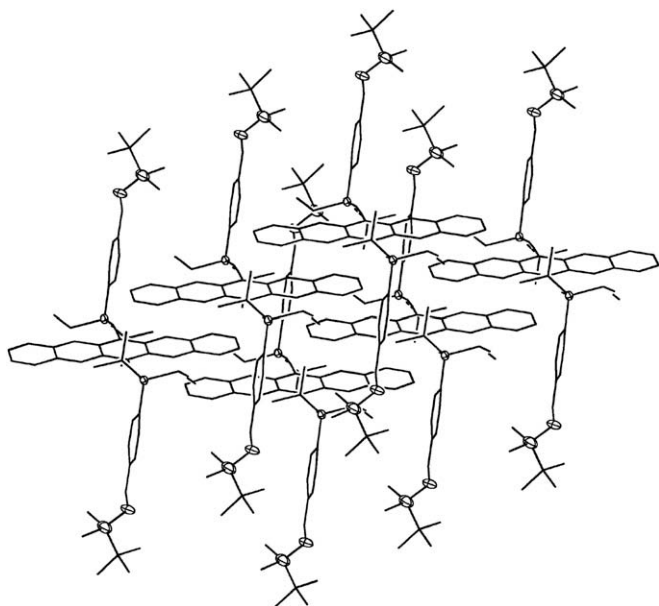


Figure 13. Solid-state arrangement of **19** (thermal ellipsoids for the carbon atoms have been omitted for clarity).

(24,400), 645 (47,100) nm. Fluorescence (CH₂Cl₂): $\lambda_{\text{exc}}=551$ nm, $\lambda_{\text{max,em}}=652$ nm, $\Phi_{\text{F}}=0.08$. IR (CDCl₃, cast) 3048 (w), 2952 (s), 2863 (s), 2136 (m), 1740 (m) cm⁻¹. ¹H NMR (500 MHz, CDCl₃): δ 9.40 (s, 4H), 9.35 (s, 4H), 8.03–7.97 (m, 8H), 7.93 (d, $J=8.0$ Hz, 4H), 7.92 (d, $J=8.1$ Hz, 4H), 7.47 (d, $J=8.2$ Hz, 4H), 7.46 (d, $J=8.2$ Hz, 4H), 7.45–7.41 (m, 8H), 5.21 (s, 4H), 4.83 (s, 4H), 2.78 (s, 4H), 1.59 (septet, $J=7.3$ Hz, 4H), 1.55 (septet, $J=7.2$ Hz, 4H), 1.42 (d, $J=7.3$ Hz, 12H), 1.40 (d, $J=7.3$ Hz, 12H), 1.29 (d, $J=7.3$ Hz, 12H), 1.26 (d, $J=7.3$ Hz, 12H), 0.98 (s, 18H), 0.14 (s, 12H). ¹³C NMR (125 MHz, CDCl₃): δ 172.1, 142.9, 137.0, 135.6, 135.3, 133.5, 132.44, 132.41, 131.43, 130.74, 130.71, 128.7, 128.6, 127.5, 126.4, 126.22, 126.18, 125.5, 118.5, 118.1, 105.9, 105.8, 105.6, 105.2, 66.5, 64.9, 29.2, 26.0, 18.4, 18.25, 18.20, 18.17, 18.13, 12.12, 12.07, –5.3 (one signal not observed). ESI MS m/z 1866.9 ([M+Na]⁺, 100). TGA: $T_{\text{d}}\approx 390$ °C. DSC: decomposition, 380 °C (onset) and 395 °C (peak).

8.4. Synthesis of trimers 35–36

As a general procedure for the synthesis of pentacene-based trimers, procedures for **36** (and its precursor compound **39**) are presented as examples. The other syntheses are analogous and details are provided in Supplementary data.

8.4.1. Synthesis of trimer **36** using DCC

Compounds **39** (0.184 g, 0.185 mmol) and **17** (0.0669 g, 0.0872 mmol) were dissolved in dry CH₂Cl₂ (5 mL), and DMAP (0.0710 g, 0.581 mmol) and DCC (0.050 g, 0.24 mmol) were added. The reaction mixture was allowed to stir at rt for 3 h before placing the flask in the refrigerator (4 °C) overnight to allow for most of the dicyclohexylurea to precipitate. The reaction mixture was filtered and the filtrate was diluted with CH₂Cl₂ (80 mL) and satd aq NaHCO₃ (200 mL). The mixture was separated and the organic phase was washed with satd aq NaHCO₃ (200 mL), 5% aq NaHCO₃ (2×200 mL), satd aq NaCl (250 mL), dried (MgSO₄), and the solvent removed in vacuo. Column chromatography (silica gel, CH₂Cl₂) afforded **36** with some residual dicyclohexylurea, which was later removed using size exclusion chromatography (BioRad Bio-Beads S-X2, 200–400 mesh, CH₂Cl₂, gravity flow) to afford **36** (0.142 g, 60%) as a deep blue solid.

8.4.2. Synthesis of trimer **36** using EDC·HCl

Compound **39** (0.160 g, 0.161 mmol), **17** (0.054 g, 0.070 mmol) and EDC·HCl (0.194 g, 1.01 mmol) were dissolved in dry CH₂Cl₂ (4 mL) and DMAP (0.148 g, 1.21 mmol) was added. The reaction mixture was allowed to stir at rt for 14 h before being poured into 5% aq NaHCO₃ (100 mL) and diluted with CH₂Cl₂ (50 mL). The mixture was separated and the organic phase was washed with 5% aq NaHCO₃ (100 mL), satd aq NaCl (150 mL), dried (MgSO₄), and the solvent removed in vacuo. Column chromatography (silica gel, CH₂Cl₂) afforded **36** (0.180 g, 94%) as a deep blue solid. $R_{\text{f}}=0.24$ (CH₂Cl₂). UV–vis (CH₂Cl₂) λ_{max} (ϵ): 271 (62,400), 309 (803,000), 330 (111,000), 440 (11,700), 551 (13,400), 594 (37,000), 645 (71,400) nm. Fluorescence (CH₂Cl₂): $\lambda_{\text{exc}}=551$ nm, $\lambda_{\text{max,em}}=652$ nm, $\Phi_{\text{F}}=0.06$. IR (CDCl₃, cast) 3048 (w), 2943 (s), 2863 (s), 2136 (m), 1739 (s) cm⁻¹. ¹H NMR (500 MHz, CDCl₃): δ 9.41 (s, 4H), 9.38 (2×s, 8H), 8.03–7.97 (m, 12H), 7.93 (m, 12H), 7.59–7.48 (m, 24H), 5.19 (s, 8H), 4.83 (s, 4H), 2.50 (t, $J=7.4$ Hz, 8H), 2.07 (quintet, $J=7.3$ Hz, 4H), 1.59 (septet, $J=7.4$ Hz, 4H), 1.56 (septet, $J=7.3$ Hz, 4H), 1.56 (septet, $J=7.1$ Hz, 4H), 1.43 (d, $J=7.2$ Hz, 12H), 1.41 (d, $J=7.3$ Hz, 12H), 1.41 (d, $J=7.3$ Hz, 12H), 1.30 (d, $J=7.4$ Hz, 12H), 1.28 (d, $J=7.4$ Hz, 12H), 1.27 (d, $J=7.3$ Hz, 12H), 0.98 (s, 18H), 0.15 (s, 12H). ¹³C NMR (125 MHz, CDCl₃): δ 172.7, 142.9, 137.16, 137.15, 135.57, 135.56, 135.3, 133.42, 133.39, 132.44, 132.43, 132.41, 131.4, 130.73, 130.70, 128.7, 128.6, 127.5, 126.4, 126.27, 126.24, 126.22, 126.18, 125.5, 118.5, 118.3, 118.1, 105.94, 105.88, 105.83, 105.6, 105.3, 105.2, 66.2, 64.9, 33.3, 26.0, 20.1, 18.4, 18.25, 18.20, 18.16, 18.13, 12.11, 12.07, –5.3 (10 signals not

observed). MALDI (CH₂Cl₂, DCTB) m/z 2721.1 ([M+H]⁺, 100). TGA: $T_{\text{d}}\approx 380$ °C. DSC: decomposition, 365 °C (onset) and 390 °C (peak).

8.4.3. Synthesis of acid **39**

Compound **18** (0.2966 g, 0.3365 mmol) and glutaric anhydride (0.150 g, 1.31 mmol) were dissolved in dry CH₂Cl₂ (7 mL) and DMAP (0.158 g, 1.29 mmol) was added. The reaction mixture was allowed to stir at rt for 2 h before being diluted with CH₂Cl₂ (70 mL) and satd aq NaHCO₃ (200 mL). The mixture was separated and the organic phase was washed with satd aq NaHCO₃ (200 mL), 5% aq NaHCO₃ (2×200 mL), satd aq NaCl (250 mL), dried (MgSO₄), and the solvent removed in vacuo. This afforded **39** (0.3324 g, 99%) as a deep blue solid. Size exclusion chromatography (BioRad Bio-Beads S-X2, 200–400 mesh, CH₂Cl₂, gravity flow) could be employed to remove traces of dimer **29** (ca. <5%) by collecting the second blue band, which elutes off the column (the first band is dimer **29**). IR (CDCl₃, cast) 3048 (w), 2952 (s), 2863 (s), 2136 (m), 1739 (s), 1710 (s) cm⁻¹. ¹H NMR (500 MHz, CDCl₃): δ 9.40 (s, 2H), 9.38 (s, 2H), 8.02–7.97 (m, 4H), 7.94 (d, $J=8.2$ Hz, 2H), 7.92 (d, $J=7.7$ Hz, 2H), 7.48–7.41 (m, 8H), 5.20 (s, 2H), 4.83 (s, 2H), 2.49 (t, $J=7.4$ Hz, 2H), 2.45 (t, $J=7.3$ Hz, 2H), 2.01 (quintet, $J=7.3$ Hz, 2H), 1.58 (septet, $J=7.3$ Hz, 4H), 1.42 (d, $J=7.3$ Hz, 12H), 1.29 (d, $J=7.3$ Hz, 12H), 0.98 (s, 9H), 0.14 (s, 6H). gCOSY NMR (500 MHz, CDCl₃): δ 9.40 ↔ 8.02–7.97; 9.38 ↔ 8.02–7.97; 8.02–7.97 ↔ 9.40, 9.38; 7.94 ↔ 7.48–7.41; 7.92 ↔ 7.48–7.41; 7.48–7.41 ↔ 8.02–7.97, 7.94, 7.92, 5.20, 4.83; 5.20 ↔ 7.48–7.40; 4.83 ↔ 7.48–7.41; 2.49 ↔ 2.01; 2.45 ↔ 2.01; 2.01 ↔ 2.45, 2.01; 1.58 ↔ 1.42, 1.29; 1.42 ↔ 1.58; 1.29 ↔ 1.58. ¹³C NMR (125 MHz, CDCl₃): δ 178.3 (br), 172.7, 142.9, 137.1, 135.6, 135.3, 133.5, 132.44, 132.42, 131.4, 130.74, 130.71, 128.7, 128.6, 127.5, 126.4, 126.23, 126.19, 125.5, 118.5, 118.1, 105.9, 105.8, 105.6, 105.2, 66.2, 64.9, 33.2, 29.7, 26.0, 19.9, 18.4, 18.25, 18.21, 18.15, 18.16, 12.11, 12.08, –5.3 (two signals not observed). ESI MS m/z 993.5 ([M–H][–], 100). ESI HRMS m/z calcd for C₆₃H₇₃O₅Si₃ ([M–H][–]) 993.4771, found 993.4758.

Acknowledgements

This work has been generously supported by the University of Alberta and the Natural Sciences and Engineering Research Council of Canada (NSERC) through the Discovery Grant program. D.L. thanks NSERC (PGS-D), the Alberta Ingenuity Fund, the University of Alberta, and the Killam Trusts for scholarship support. We thank Prof. Robert E. Campbell (University of Alberta) for helpful discussions regarding fluorescence spectroscopy.

Supplementary data

Experimental procedures and spectroscopic data for compounds **15–20** and **22–39**, MS spectra for polymers, UV–vis spectra of thin films of the polymers, and graph of molar absorptivity as a function of number of pentacene units. Supplementary data associated with this article can be found in the online version, at doi:10.1016/j.tet.2008.09.041.

References and notes

- For recent reviews on acenes, see: (a) Bendikov, M.; Wudl, F.; Perepichka, D. F. *Chem. Rev.* **2004**, *104*, 4891–4945; (b) Anthony, J. E. *Chem. Rev.* **2006**, *106*, 5028–5048; (c) Anthony, J. E. *Angew. Chem., Int. Ed.* **2008**, *47*, 452–483.
- Murphy, A. R.; Fréchet, J. M. J. *Chem. Rev.* **2007**, *107*, 1066–1096.
- Briseno, A. L.; Mannsfeld, S. C. B.; Jenekhe, S. A.; Bao, Z.; Xia, Y. *Mater. Today* **2008**, *11* (4), 38–47.
- For recent examples, see: (a) Anthony, J. E.; Brooks, J. S.; Eaton, D. L.; Parkin, S. R. *J. Am. Chem. Soc.* **2001**, *123*, 9482–9483; (b) Anthony, J. E.; Eaton, D. L.; Parkin, S. R. *Org. Lett.* **2002**, *4*, 15–18; (c) Payne, M. M.; Delcamp, J. H.; Parkin, S. R.; Anthony, J. E. *Org. Lett.* **2004**, *6*, 1609–1612; (d) Payne, M. M.; Odom, S. A.; Parkin, S. R.; Anthony, J. E. *Org. Lett.* **2004**, *6*, 3325–3328; (e) Swartz, C. R.; Parkin, S. R.; Bullock, J. E.; Anthony, J. E.; Mayer, A. C.; Malliaras, G. G. *Org. Lett.* **2005**, *7*, 3163–3166; (f) Susumu, K.; Duncan, T. V.; Therien, M. J. *J. Am. Chem.*

- Soc. **2005**, 127, 5186–5195; (g) Vets, N.; Smet, M.; Dehaen, W. *Synlett* **2005**, 217–222; (h) Chan, S. H.; Lee, H. K.; Wang, Y. M.; Fu, N. Y.; Chen, X. M.; Cai, Z. W.; Wong, H. N. C. *Chem. Commun.* **2005**, 66–68; (i) Takahashi, T.; Li, S.; Huang, W.; Kong, F.; Nakajima, K.; Shen, B.; Ohe, T.; Kanno, K.-i. *J. Org. Chem.* **2006**, 71, 7967–7977; (j) Briseno, A. L.; Miao, Q.; Ling, M.-M.; Reese, C.; Meng, H.; Bao, Z.; Wudl, F. *J. Am. Chem. Soc.* **2006**, 128, 15576–15577; (k) Miao, Q.; Chi, X.; Xiao, S.; Zeis, R.; Lefenfeld, M.; Siegrist, T.; Steigerwald, M. L.; Nuckolls, C. *J. Am. Chem. Soc.* **2006**, 128, 1340–1345; (l) Palayangoda, S. S.; Mondal, R.; Shah, B. K.; Neckers, D. C. *J. Org. Chem.* **2007**, 72, 6584–6587; (m) Chen, J.; Subramanian, S.; Parkin, S. R.; Siegler, M.; Gallup, K.; Haughn, C.; Martin, D. C.; Anthony, J. E. *J. Mater. Chem.* **2008**, 18, 1961–1969; (n) For supramolecular assemblies, see: Desvergne, J.-P.; Del Guerso, A.; Bouas-Laurent, H.; Belin, C.; Reichwagen, J.; Hopf, H. *Pure Appl. Chem.* **2006**, 78, 707–719.
5. A preliminary account of this work has appeared: Lehnher, D.; Tykwinski, R. R. *Org. Lett.* **2007**, 9, 4583–4586.
6. Ito, K.; Suzuki, T.; Sakamoto, Y.; Kubota, D.; Inoue, Y.; Sato, F.; Tokito, S. *Angew. Chem., Int. Ed.* **2003**, 42, 1159–1162.
7. Dell'Aquila, A.; Marinelli, F.; Tey, J.; Keg, P.; Lam, Y.-M.; Kapitanchuk, O. L.; Mastroianni, P.; Nobile, C. F.; Cosma, P.; Marchenko, A.; Fichou, D.; Mhaisalkar, S. G.; Suranna, G. P.; Torsi, L. *J. Mater. Chem.* **2008**, 18, 786–791.
8. Merlo, J. A.; Newman, C. R.; Gerlach, C. P.; Kelley, T. W.; Muires, D. V.; Fritz, S. E.; Toney, M. F.; Frisbie, C. D. *J. Am. Chem. Soc.* **2005**, 127, 3997–4009.
9. (a) Toyota, S.; Goichi, M.; Kotani, M. *Angew. Chem., Int. Ed.* **2004**, 43, 2248–2251; (b) Toyota, S.; Kurokawa, M.; Araki, M.; Nakamura, K.; Iwanaga, T. *Org. Lett.* **2007**, 9, 3655–3658.
10. Akiyama, S.; Misumi, S.; Nakagawa, M. *Bull. Chem. Soc. Jpn.* **1960**, 33, 1293–1298.
11. Zhao, W.; Tang, Q.; Chan, H. S.; Xu, J.; Lo, K. Y.; Miao, Q. *Chem. Commun.* **2008**, 4324–4326.
12. Tokito, S.; Weinfurter, K.-H.; Fujikawa, H.; Tsutsui, T.; Taga, Y. *Proc. SPIE-Int. Soc. Opt. Eng.* **2001**, 4105, 69–74.
13. Okamoto, T.; Bao, Z. *J. Am. Chem. Soc.* **2007**, 129, 10308–10309.
14. The term pro-cata positions on pentacene was defined in the following reference: Anthony, J. E.; Gierschner, J.; Landis, C. A.; Parkin, S. R.; Sherman, J. B.; Bakus, R. C., II. *Chem. Commun.* **2007**, 4746–4748.
15. Lehnher, D.; Gao, J.; Hegmann, F. A.; Tykwinski, R. R. *Org. Lett.* **2008**. doi: 10.1021/ol801886h
16. Sessler, J. L.; Wang, B.; Harriman, A. *J. Am. Chem. Soc.* **1995**, 117, 704–714.
17. See **Supplementary data** for mass spectra of polymers and a more detailed discussion.
18. Goodings, E. P.; Mitchard, D. A.; Owen, G. *J. Chem. Soc., Perkin Trans. 1* **1972**, 1310–1314.
19. Maulding, D. R.; Roberts, B. G. *J. Org. Chem.* **1969**, 34, 1734–1736.
20. See **Supplementary data** for graphs.
21. See **Supplementary data** for solid-state spectra.
22. Isak, S. J.; Eyring, E. M. *J. Phys. Chem.* **1992**, 96, 1738–1742.
23. (a) Sibilina, J. P. *A Guide to Materials Characterization and Chemical Analysis*; VCH: New York, NY, 1988; (b) Kämpf, G. *Characterization of Plastics by Physical Methods: Experimental Techniques and Practical Applications*; Hanser: New York, NY, 1986.
24. Lehnher, D.; McDonald, R.; Tykwinski, R. R. *Org. Lett.* **2008**, 10, 4163–4166.
25. X-ray crystallographic data for **17**·2MeOH: C₅₂H₅₄O₂Si₂·2CH₃OH, *M*=831.22; monoclinic space group *P*2₁/*c* (No. 14); $\rho_{\text{calcd}}=1.156\text{ g cm}^{-3}$; $a=8.8223(6)\text{ \AA}$, $b=19.0409(13)\text{ \AA}$, $c=14.6224(10)\text{ \AA}$; $\beta=103.5400(16)^\circ$; $V=2388.1(3)\text{ \AA}^3$; $Z=2$; $\mu=0.118\text{ mm}^{-1}$. Final $R_1(F)=0.0433$ (6400 observations [$F_o^2 \geq 2\sigma(F_o^2)$]); $wR_2(F^2)=0.0985$ for 275 variables and 10,024 data with [$F_o^2 \geq -3\sigma(F_o^2)$]; CCDC 654502. X-ray data have been deposited at the Cambridge Crystallographic Data Centre, 12 Union Road, Cambridge CB21EZ, UK; fax: (+44)122 333 6033.
26. For acene solid-state packing terminology, see: Ref. **1b**.
27. The interplanar distance was obtained by defining a mean-square plane from the 22 pentacene carbons and measuring the distance to the adjacent acene plane.
28. X-ray crystallographic data for **17**·acetone: C₅₂H₅₄O₂Si₂·(CH₃)₂CO, *M*=825.21; monoclinic space group *P*2₁/*c* (No. 14); $\rho_{\text{calcd}}=1.144\text{ g cm}^{-3}$; $a=8.9392(9)\text{ \AA}$, $b=52.448(5)\text{ \AA}$, $c=15.6959(16)\text{ \AA}$; $\beta=102.5066(16)^\circ$; $V=7184.3(13)\text{ \AA}^3$; $Z=6$; $\mu=0.116\text{ mm}^{-1}$. Final $R_1(F)=0.0728$ (11,705 observations [$F_o^2 \geq 2\sigma(F_o^2)$]); $wR_2(F^2)=0.1841$ for 812 variables and 14,079 data with [$F_o^2 \geq -3\sigma(F_o^2)$]; CCDC 697879.
29. X-ray crystallographic data for **19**: C₆₄H₈₂O₂Si₄, *M*=995.66; triclinic space group *P*1 (No. 2); $\rho_{\text{calcd}}=1.111\text{ g cm}^{-3}$; $a=7.3144(7)\text{ \AA}$, $b=78.8444(8)\text{ \AA}$, $c=26.168(3)\text{ \AA}$; $\alpha=89.717(2)^\circ$, $\beta=183.279(2)^\circ$, $\gamma=86.803(2)^\circ$; $V=1488.8(3)\text{ \AA}^3$; $Z=1$; $\mu=0.141\text{ mm}^{-1}$. Final $R_1(F)=0.0934$ (3021 observations [$F_o^2 \geq 2\sigma(F_o^2)$]); $wR_2(F^2)=0.2937$ for 397 variables, 49 restraints, and 5245 data with [$F_o^2 \geq -3\sigma(F_o^2)$]; CCDC 697880. The *t*-BuMe₂SiOCH₂C₆H₄ side chain exhibited disorder over two positions in which both components were 50% occupied. The more poorly behaved component was restrained to have the same geometry (distances and angles) as the better behaved one by use of the SHELXL instruction SAME. Additionally, the *t*-butyl group of the better behaved orientation was restrained to have the same Me–C bond distances. Finally, equivalent atoms between the *t*-BuMe₂Si groups were constrained to have the same anisotropic displacement parameters.
30. (a) Sheraw, C. D.; Jakson, T. N.; Eaton, D. L.; Anthony, J. E. *Adv. Mater.* **2003**, 15, 2009–2011; (b) Subramanian, S.; Park, S. K.; Parkin, S. R.; Podzorov, V.; Jackson, T. N.; Anthony, J. E. *J. Am. Chem. Soc.* **2008**, 130, 2706–2707.
31. Ried, W.; Anthöfer, F. *Angew. Chem.* **1953**, 65, 601.